

Yusuke Nishida · Shina Tan

# Liberating Efimov physics from three dimensions

April 2011

**Abstract** When two particles attract via a resonant short-range interaction, three particles always form an infinite tower of bound states characterized by a discrete scaling symmetry. It has been considered that this Efimov effect exists only in three dimensions. Here we review how the Efimov physics can be liberated from three dimensions by considering two-body and three-body interactions in mixed dimensions and four-body interaction in one dimension. In such new systems, intriguing phenomena appear, such as confinement-induced Efimov effect, Bose-Fermi crossover in Efimov spectrum, and formation of interlayer Efimov trimers. Some of them are observable in ultracold atom experiments and we believe that this study significantly broadens our horizons of universal Efimov physics.

## Contents

1	Introduction . . . . .	2
2	Absence of Efimov effect in other than three dimensions . . . . .	2
3	Unitarity interactions beyond three dimensions . . . . .	4
4	Efimov physics beyond three dimensions . . . . .	5
4.1	Confinement-induced Efimov effect . . . . .	5
4.2	Bose-Fermi crossover in Efimov spectrum . . . . .	8
4.3	Interlayer Efimov trimers and stability in ultracold atoms . . . . .	9
4.4	Resonantly interacting anyons in two dimensions . . . . .	11
5	Summary . . . . .	12
A	Details of Bose-Fermi crossover in 1D-3D mixture . . . . .	12
B	Details of interlayer and interwire Efimov trimers . . . . .	14
B.1	Bilayer 2D-3D mixture . . . . .	14
B.2	Biwire 1D-3D mixture . . . . .	15

---

Special issue devoted to Efimov physics

---

Yusuke Nishida  
Center for Theoretical Physics, Massachusetts Institute of Technology, Cambridge, MA 02139, USA  
E-mail: nishida@mit.edu

Shina Tan  
School of Physics, Georgia Institute of Technology, Atlanta, GA 30332, USA  
E-mail: shina.tan@physics.gatech.edu

## 1 Introduction

When particles attract via a short-range two-body interaction whose  $s$ -wave scattering length is much larger than the range of the interaction potential, their low-energy physics becomes *universal*, i.e., independent of details of the interaction potential [1]. In 1970, Vitaly Efimov discovered that three particles at infinite scattering length form an infinite tower of bound states whose binding energies  $E_n$  have an accumulation point at  $E = 0$  [2]. The most important characteristic of this Efimov effect is the existence of a discrete scaling symmetry. Namely, the ratio of two successive binding energies is constant

$$\frac{E_{n+1}}{E_n} = \lambda^{-2} \quad (1)$$

where  $\lambda$  is a scaling factor and given by  $\lambda = 22.7$  for three identical bosons. This discrete scaling symmetry is descended from the full scaling symmetry of the zero-range two-body interaction at infinite scattering length. The necessity to regularize the short-distance behavior of three particles breaks the full scaling symmetry down to a discrete one and leads to the infinite tower of bound states. This peculiar phenomenon is a rare manifestation of the renormalization group limit cycle in physics [3]. In this article, *we define the Efimov effect as the appearance of an infinite tower of bound states with a discrete scaling symmetry when particles attract via short-range interactions.*

After the discovery by Efimov, it has been repeatedly discussed that the Efimov effect is absent in two dimensions [4,5,6,7,8,9,10]. More precisely, the Efimov effect for three identical bosons appears only in an interval of  $2.30 < d < 3.76$  [11]. Why does the Efimov effect exist only in three dimensions? Or, can we liberate the universal Efimov physics from three dimensions? More generally, when does such a peculiar phenomenon appear? These are questions we would like to address in this article.

In Sect. 2, we provide a simple argument to understand the absence of the Efimov effect in other than three dimensions. Our logic is such that *in order for the Efimov effect to appear, it is necessary that particles attract via scale-invariant interactions* from the definition of the Efimov effect. However, short-range two-body interactions can satisfy this necessary condition only in three dimensions. Therefore, the key to liberate the Efimov physics from three dimensions is whether we can find scale-invariant short-range interactions in other than three dimensions. In Sect. 3, we show that two-body and three-body interactions in mixed dimensions and four-body interaction in one dimension can be scale invariant at their resonances and thus they satisfy the necessary condition for the Efimov effect. All such new systems indeed exhibit the Efimov effect as we will show in a separate paper [12]. Table 1 summarizes a part of our results on the presence of the Efimov effect and critical mass ratios in various three-body systems with resonant two-body interactions. In Sect. 4, we discuss a number of universal phenomena unique in such new systems and observable in ultracold atom experiments. Section 5 is the summary of this article and some details of results discussed in the text are presented in Appendices. In view of the fact that most studies on the Efimov effect have been devoted to three dimensions for more than 40 years, we believe that this study significantly broadens our horizons of universal Efimov physics.

## 2 Absence of Efimov effect in other than three dimensions

Suppose two particles interact via a short-range potential  $V(\mathbf{r})$  that vanishes outside its potential range;  $V(|\mathbf{r}| > r_0) = 0$ . After separating the center-of-mass motions, the two-body scattering is described by

**Table 1** Efimov effect in  $AAB$  systems with resonant two-body interactions between  $A$  and  $B$  particles in pure 3D, 2D-3D, 1D-3D, 2D-2D, and 1D-2D mixtures.  $\circ$  ( $\times$ ) indicates the presence (absence) of the Efimov effect for any mass ratio  $m_A/m_B$ , while numbers indicate critical mass ratios above which the Efimov effect appears.

$B \backslash A$	3D		2D		1D	
	boson	fermion	boson	fermion	boson	fermion
3D	$\circ$	13.6	$\circ$	6.35	$\circ$	2.06
2D	$\circ$	28.5	$\circ$	11.0	$\circ$	$\times$
1D	$\circ$	155	$\circ$	$\times$	—	

the three-dimensional Schrödinger equation

$$\left[ -\frac{\hbar^2}{2\mu} \frac{\partial^2}{\partial \mathbf{r}^2} + V(\mathbf{r}) \right] \psi(\mathbf{r}) = E \psi(\mathbf{r}) \quad \text{with} \quad \mathbf{r} = (r_1, r_2, r_3), \quad (2)$$

where  $\mu$  is the reduced mass. The relative wave function outside the potential range but at the distance scale much shorter than the de Broglie wavelength,  $r_0 < |\mathbf{r}| \ll \hbar/\sqrt{2\mu E}$ , obeys the Laplace's equation

$$\frac{\partial^2}{\partial \mathbf{r}^2} \psi(\mathbf{r}) = 0. \quad (3)$$

The general solution to this equation in the  $s$ -wave channel is given by

$$\psi(\mathbf{r}) \propto \frac{1}{|\mathbf{r}|} - \frac{1}{a}, \quad (4)$$

where  $a$  is the  $s$ -wave scattering length. The scattering length becomes infinite  $a \rightarrow \infty$  at the resonance where the interaction potential supports a two-body bound state exactly at zero binding energy. Furthermore, if we are interested in the low-energy physics whose de Broglie wavelength is much longer than the potential range  $r_0 \ll \hbar/\sqrt{2\mu E}$ , we can regard such a short-range potential as a zero-range potential. The scale invariance is achieved by taking the zero-range limit  $r_0 \rightarrow 0$  with keeping the scattering length infinite. Now the Schrödinger equation becomes

$$-\frac{\hbar^2}{2\mu} \frac{\partial^2}{\partial \mathbf{r}^2} \psi(\mathbf{r}) = E \psi(\mathbf{r}) \quad \text{for} \quad |\mathbf{r}| \neq 0 \quad (5)$$

and the interaction potential is replaced by the short-range boundary condition:

$$\psi(|\mathbf{r}| \rightarrow 0) \propto \frac{1}{|\mathbf{r}|} + O(|\mathbf{r}|). \quad (6)$$

Then by adding a third particle, one can show that the Efimov effect appears [2]. Our purpose here is not to show the presence of the Efimov effect in three dimensions but to show the presence of the scale-invariant interaction, which is necessary for the Efimov effect. We refer to the zero-range and infinite scattering length interaction implemented by Eq. (6) (and its analytic continuation to other spatial dimensions) as the unitarity interaction.

In order to understand the absence of the Efimov effect in other than three dimensions, we generalize the above argument to arbitrary spatial dimensions. In  $D$  dimensions, the short-range boundary condition (6) is modified as

$$\psi(|\mathbf{r}| \rightarrow 0) \propto \frac{1}{|\mathbf{r}|^{D-2}} + O(|\mathbf{r}|^{4-D}, |\mathbf{r}|^2), \quad (7)$$

which is the singular solution to the  $D$ -dimensional Laplace's equation (3). Because the wave function has to be normalizable, the singularity of the wave function in Eq. (7) is unacceptable in higher dimensions  $D > 4$ . In  $D = 4$ , the normalization integral is logarithmically divergent at the origin which implies that two particles behave as a point-like composite particle [13,14]. This composite particle is noninteracting with a third particle and thus they cannot form bound states. On the other hand, the singularity of the wave function disappears in  $D = 2$  which means that the interaction between two particles also disappears. Obviously, three particles cannot form bound states from no interaction. Finally in  $D = 1$ , the wave function (7) behaves as  $\psi(|\mathbf{r}|) \propto |\mathbf{r}|$  at the short distance, which is a consequence of the hardcore repulsion between two particles. The hardcore repulsion is scale invariant but three particles cannot form bound states from the repulsive interaction. Indeed, the spectrum of particles interacting via the hardcore repulsion in  $D = 1$  is equivalent to that of noninteracting identical fermions [15]. Therefore, we find that the Efimov effect cannot appear in one, two, and four dimensions from any short-range two-body interactions because the unitarity interaction becomes trivial in such dimensions. Table 2 summarizes the fate of three identical bosons in the unitarity limit as a function of the dimensionality  $D$ .

**Table 2** Fate of three identical bosons in the unitarity limit. They form an Efimov trimer only in  $D = 3$  and become trivial systems in  $D = 1, 2, 4$ . The unitarity interaction does not exist in higher dimensions  $D > 4$ .

$D = 1$	hardcore repulsion $\Rightarrow$ free fermions
$D = 2$	free bosons
$D = 3$	<b>Efimov trimer</b> ( $2.30 < d < 3.76$ )
$D = 4$	free composite + one boson

For completeness, we also consider higher partial-wave interactions. In a partial-wave channel with orbital angular momentum  $\ell \geq 0$ , the radial wave function at the distance scale  $r_0 < |\mathbf{r}| \ll \hbar/\sqrt{2\mu E}$  behaves as

$$\psi(\mathbf{r}) \propto \frac{1}{|\mathbf{r}|^{\ell+D-2}} - \frac{|\mathbf{r}|^\ell}{a_\ell}. \quad (8)$$

In order for the interaction potential to produce the scale-invariant attraction in the zero-range limit  $r_0 \rightarrow 0$ , the power of the first term needs to satisfy

$$0 < \ell + D - 2 < \frac{D}{2}. \quad (9)$$

The first inequality comes from the requirement of the attraction and the second comes from the normalizability of the wave function. The constraint (9) cannot be satisfied by any non-negative integers  $\ell = 0, 1, 2, \dots$  in  $D \geq 4$ , while it can be satisfied only in the  $s$ -wave channel  $\ell = 0$  in  $D = 3$  that is the case discussed above. In  $D = 2$ , Eq. (9) reduces to  $0 < \ell < 1$ , which cannot be satisfied by bosons ( $\ell = 0$ ) or fermions ( $\ell = 1$ ) but can be satisfied by anyons [16]. The case of anyons will be treated separately in Sect. 4.4.

### 3 Unitarity interactions beyond three dimensions [17]

We have seen that the Efimov effect can appear only in three dimensions because the scale-invariant unitarity interaction is nontrivial only in three dimensions and becomes trivial in one, two, and four dimensions and does not exist in higher dimensions. Therefore, the key to liberate the Efimov physics from three dimensions is whether we can find nontrivial scale-invariant short-range interactions in other than three dimensions. We recall that three dimensions were special because the relative wave function at a short distance obeys the three-dimensional Laplace's equation (3) that admits the normalizable singular solution as in Eq. (6). However, three spatial dimensions are actually not essential for the three-dimensional Laplace's equation. What is essential is the fact that the scattering is described by three relative coordinates  $\mathbf{r} = (r_1, r_2, r_3)$  and their physical meaning does not matter. Of course, as far as the scattering of two particles living in the same space is concerned, the numbers of spatial dimensions and relative coordinates coincide, but more generally they do not. For example, the scattering of four particles in one dimension is described by the same Schrödinger equation as Eq. (2) with three relative coordinates  $\mathbf{r} = (r_1, r_2, r_3)$  because each particle has one coordinate and one center-of-mass coordinate can be separated. The short-range potential  $V(\mathbf{r})$  in this case represents a four-body interaction in one dimension, which produces the scale-invariant attraction in the zero-range limit at the four-body resonance.

In order to elucidate all possible scale-invariant short-range interactions, we consider the scattering of  $N$  particles labeled by  $i = 1, \dots, N$ , each of which lives in a  $d_i$ -dimensional flat space. If all spaces have a common  $d_{\parallel}$ -dimensional intersection, the center-of-mass motions in such directions can be separated from the relative motions. Therefore, by introducing the codimension  $d_{\perp i} \equiv d_i - d_{\parallel}$ , the number of relative coordinates is given by

$$D = \sum_{i=1}^N d_i - d_{\parallel} = \sum_{i=1}^N d_{\perp i} + (N - 1) d_{\parallel} \quad (10)$$

**Table 3** All possible combinations of spatial dimensions  $d_i \geq 1$  where the scattering of  $N$  particles is described by three relative coordinates [17]. In each system, an  $N$ -body interaction potential becomes scale invariant in the unitarity limit and  $N+1$  particles exhibit the Efimov effect.

# of particles and dimensions	Name	Example of geometry
$N = 2$ $(d_A, d_B; d_{\parallel}) = (3, 3; 3)$	pure 3D	$\mathbf{x}_A = \mathbf{x}_B = (x, y, z)$
$N = 2$ $(d_A, d_B; d_{\parallel}) = (2, 3; 2)$	2D-3D mixture	$\mathbf{x}_A = (x, y)$ $\mathbf{x}_B = (x, y, z)$
$N = 2$ $(d_A, d_B; d_{\parallel}) = (1, 3; 1)$	1D-3D mixture	$\mathbf{x}_A = (z)$ $\mathbf{x}_B = (x, y, z)$
$N = 2$ $(d_A, d_B; d_{\parallel}) = (2, 2; 1)$	2D-2D mixture	$\mathbf{x}_A = (x, z)$ $\mathbf{x}_B = (y, z)$
$N = 2$ $(d_A, d_B; d_{\parallel}) = (1, 2; 0)$	1D-2D mixture	$\mathbf{x}_A = (z)$ $\mathbf{x}_B = (x, y)$
$N = 3$ $(d_A, d_B, d_C; d_{\parallel}) = (1, 1, 2; 1)$	1D <sup>2</sup> -2D mixture	$\mathbf{x}_A = \mathbf{x}_B = (x)$ $\mathbf{x}_C = (x, y)$
$N = 3$ $(d_A, d_B, d_C; d_{\parallel}) = (1, 1, 1; 0)$	1D-1D-1D mixture	$\mathbf{x}_A = (x)$ $\mathbf{x}_B = (y)$ $\mathbf{x}_C = (z)$
$N = 4$ $(d_A, d_B, d_C, d_D; d_{\parallel}) = (1, 1, 1, 1; 1)$	pure 1D	$\mathbf{x}_A = \mathbf{x}_B = \mathbf{x}_C = \mathbf{x}_D = (x)$

and the scattering problem is described by the  $D$ -dimensional Schrödinger equation (2). If  $d_{\perp i} = 0$  for all  $i$ , all particles live in the same space while otherwise they live in different spaces and interact only at their intersection. The latter case is referred to as *mixed dimensions*. As we have shown, the short-range  $N$ -body interaction potential  $V(\mathbf{r})$  can produce the scale-invariant attraction in the unitarity limit only when  $D = 3$ . All possible combinations of spatial dimensions for  $D = 3$  are summarized in Table 3. Here we assumed  $d_i \geq 1$  for all  $i$  because  $d_i = 0$  corresponds a zero-dimensional impurity and is rather trivial. In addition to the ordinary two-body interaction in three dimensions, we find seven more systems in which short-range few-body interactions become scale invariant in the unitarity limit; two-body and three-body interactions in mixed dimensions and four-body interaction in one dimension [17]. These new systems in the unitarity limit satisfy the necessary condition for the Efimov effect and thus we expect that the addition of an  $(N+1)$ th particle may lead to the formation of an infinite tower of  $(N+1)$ -body bound states with a discrete scaling symmetry. Indeed, this expectation turns out to be true and  *$N+1$  particles in all such new systems exhibit the Efimov effect* as we will show in a separate paper [12]. By this way, we can liberate the universal Efimov physics from three dimensions!

#### 4 Efimov physics beyond three dimensions

We shall defer to Ref. [12] on complete and unified analyses of the Efimov effect in all possible cases found in the previous section. Instead, here we focus on a number of universal phenomena that cannot be found in the ordinary Efimov physics in three dimensions and are thus unique in our new systems. Some of them are observable in ultracold atom experiments.

##### 4.1 Confinement-induced Efimov effect [18]

Let us consider a three-body system composed of two  $A$  and one  $B$  particles in which  $A$  and  $B$  particles attract via a zero-range and infinite scattering length interaction while two  $A$  particles do not interact with each other. The presence or absence of the Efimov effect can be diagnosed by studying the scaling behavior of three-body wave function  $\psi \sim R^{\gamma_\ell}$  at a small hyperradius  $R \rightarrow 0$  in a given partial-wave channel classified by a quantum number  $\ell$ .<sup>1</sup> When the scaling exponent  $\gamma_\ell$  develops an imaginary part  $\text{Im}[\gamma_\ell] \equiv s_\ell > 0$ , the Efimov effect appears in the  $\ell$ th partial-wave channel<sup>2</sup> and the spectrum of  $AAB$

<sup>1</sup> For example,  $\ell = 0, 1, 2, \dots$  is the orbital angular momentum in pure 3D,  $\ell = 0, \pm 1, \pm 2, \dots$  is the magnetic quantum number in 2D-3D mixture, and  $(-1)^\ell = \pm 1$  ( $\ell = 0, 1$ ) is the parity in 1D-3D mixture.

<sup>2</sup> On the other hand, real solutions of the scaling exponent  $\gamma_\ell$  correspond to energies of  $N+1$  particles in a harmonic potential by  $E = \left(\frac{1}{2} \sum_{i=1}^{N+1} d_i + \gamma_\ell + 2n\right) \hbar\omega$  with  $n = 0, 1, 2, \dots$  [19, 20, 21].

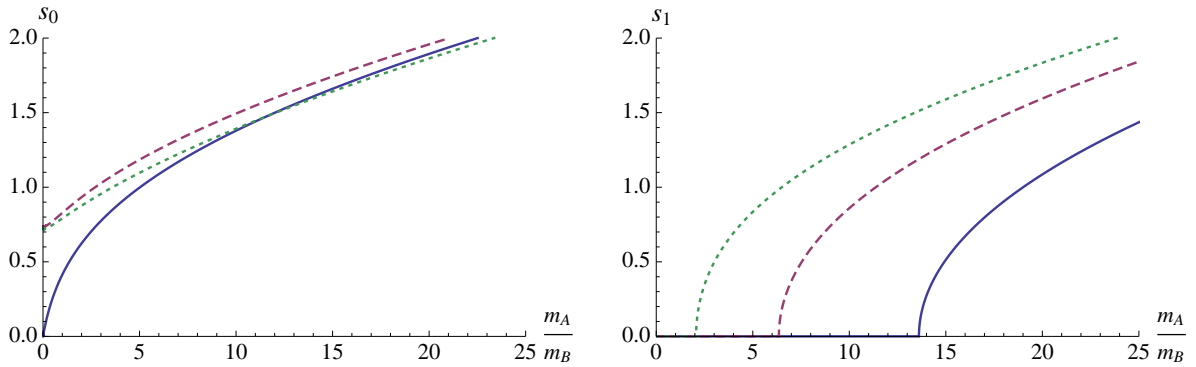


**Fig. 1** Exponents  $s_\ell$  of  $AAB$  Efimov trimers as functions of the mass ratio  $m_A/m_B$  when  $A$  particles are bosons (left) and fermions (right). Solid, dashed, and dotted curves correspond to pure 3D, 2D-3D mixture, and 1D-3D mixture, respectively, in which two  $A$  particles are confined in lower dimensions and resonantly interact with one  $B$  particle in 3D. Scaling factors are given by  $\lambda = e^{\pi/s_\ell}$  and  $s_\ell = 0$  indicates the absence of the Efimov effect.

Efimov trimers exhibits the discrete scaling symmetry as in Eq. (1):

$$\frac{E_{n+1}}{E_n} = e^{-2\pi/s_\ell} \equiv \lambda^{-2}. \quad (11)$$

Here the scaling factor  $\lambda = e^{\pi/s_\ell} > 1$  depends on the mass ratio  $m_A/m_B$ , statistics, and dimensionality of  $A$  and  $B$  particles. Figure 1 shows the exponent  $s_\ell$  as a function of  $m_A/m_B$  in pure 3D, 2D-3D mixture, and 1D-3D mixture, in which two  $A$  particles are confined in lower dimensions with keeping one  $B$  particle in 3D [17]. When  $s_\ell$  is larger (smaller), the spectrum becomes denser (sparser) and  $s_\ell = 0$  indicates the absence of the Efimov effect.

When  $A$  particles are bosons (left panel in Fig. 1), the  $AAB$  system always exhibits the Efimov effect in the  $s$ -wave or even-parity channel ( $\ell = 0$ ) for any mass ratio, but the scaling factor is strongly affected by the dimensionality of  $A$  particles. For example, for  $m_A/m_B = 87/41$  corresponding to the Bose-Bose mixture of  $A = {}^{87}\text{Rb}$  and  $B = {}^{41}\text{K}$  [22], the scaling factor is given by

$$\lambda = 131 \quad \text{in pure 3D,} \quad (12a)$$

$$\lambda = 27.7 \quad \text{in 2D-3D mixture,} \quad (12b)$$

$$\lambda = 34.6 \quad \text{in 1D-3D mixture,} \quad (12c)$$

while for  $m_A/m_B = 41/87$  corresponding to  $A = {}^{41}\text{K}$  and  $B = {}^{87}\text{Rb}$ , we find

$$\lambda = 3.48 \times 10^5 \quad \text{in pure 3D,} \quad (13a)$$

$$\lambda = 59.3 \quad \text{in 2D-3D mixture,} \quad (13b)$$

$$\lambda = 67.6 \quad \text{in 1D-3D mixture.} \quad (13c)$$

Therefore, the scaling factor can be significantly decreased by confining two  $A$  particles in lower dimensions, which makes the spectrum of  $AAB$  Efimov trimers much denser.

On the other hand, when  $A$  particles are fermions (right panel in Fig. 1), the effect of the confinement is more striking. As a consequence of the Fermi statistics, there is a critical mass ratio above which the  $AAB$  system exhibits the Efimov effect in the  $p$ -wave or odd-parity channel ( $\ell = 1$ ) [23]. The critical mass ratio depends on the dimensionality of  $A$  particles and is given by

$$m_A/m_B = 13.6 \quad \text{in pure 3D,} \quad (14a)$$

$$m_A/m_B = 6.35 \quad \text{in 2D-3D mixture,} \quad (14b)$$

$$m_A/m_B = 2.06 \quad \text{in 1D-3D mixture.} \quad (14c)$$

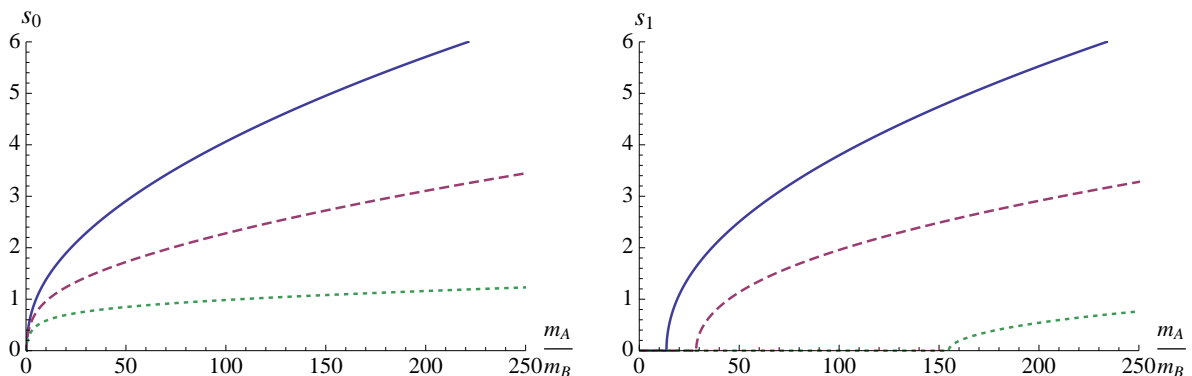


**Fig. 2** Same as Fig. 1 but for cases in which one  $B$  particle is confined in lower dimensions and resonantly interacts with two  $A$  particles in 3D.

Therefore, although the Fermi-Fermi mixture of  $A = {}^{40}\text{K}$  and  $B = {}^6\text{Li}$  with  $m_A/m_B = 40/6$  does not exhibit the Efimov effect in a free space, the Efimov effect can be induced by confining two  ${}^{40}\text{K}$  atoms in lower dimensions because their mass ratio lies in  $6.35 < m_A/m_B < 13.6$ . The scaling factor in this case is given by

$$\text{no Efimov effect} \quad \text{in pure 3D,} \quad (15a)$$

$$\lambda = 1.78 \times 10^5 \quad \text{in 2D-3D mixture,} \quad (15b)$$

$$\lambda = 22.0 \quad \text{in 1D-3D mixture.} \quad (15c)$$

This is a new type of the Efimov effect referred to as *confinement-induced Efimov effect* and will be observable in ultracold atom experiments [24, 25, 26, 27, 28, 29, 30] through the measurement of the three-body recombination rate [18]. As is discussed in Refs. [18, 31], resulting Efimov trimers realized in ultracold atoms have a small decay width and thus they are expected to be long-lived. On the other hand, for  $m_A/m_B = 6/40 < 2.06$  corresponding to  $A = {}^6\text{Li}$  and  $B = {}^{40}\text{K}$ , the Efimov effect does not take place in any dimensions.

Figure 2 shows the same exponent  $s_\ell$  but for cases in which one  $B$  particle is confined in lower dimensions with keeping two  $A$  particles in 3D [17]. When  $A$  particles are bosons (left panel in Fig. 2), the  $AAB$  system always exhibits the Efimov effect in the  $s$ -wave or even-parity channel ( $\ell = 0$ ) for any mass ratio  $m_A/m_B$ , but the scaling factor  $\lambda = e^{\pi/s_\ell}$  is significantly increased by the confinement. For example, for  $m_A/m_B = 87/41$  or  $m_A/m_B = 41/87$ , we find

$$\lambda = 131 \quad \text{or} \quad \lambda = 3.48 \times 10^5 \quad \text{in pure 3D,} \quad (16a)$$

$$\lambda = 529 \quad \text{or} \quad \lambda = 6.95 \times 10^6 \quad \text{in 2D-3D mixture,} \quad (16b)$$

$$\lambda = 1.10 \times 10^4 \quad \text{or} \quad \lambda = 5.67 \times 10^9 \quad \text{in 1D-3D mixture,} \quad (16c)$$

respectively. On the other hand, when  $A$  particles are fermions (right panel in Fig. 2), the  $AAB$  system exhibits the Efimov effect in the  $p$ -wave or odd-parity channel ( $\ell = 1$ ) only above a critical mass ratio given by

$$m_A/m_B = 13.6 \quad \text{in pure 3D,} \quad (17a)$$

$$m_A/m_B = 28.5 \quad \text{in 2D-3D mixture,} \quad (17b)$$

$$m_A/m_B = 155 \quad \text{in 1D-3D mixture.} \quad (17c)$$

Therefore, the formation of  $AAB$  Efimov trimers becomes more difficult by confining one  $B$  particle in lower dimensions as opposed to confining two  $A$  particles. In particular, this Efimov effect does not take place in any dimensions for the Fermi-Fermi mixture of  $A = {}^{40}\text{K}$ ,  $B = {}^6\text{Li}$  or  $A = {}^6\text{Li}$ ,  $B = {}^{40}\text{K}$ .

## 4.2 Bose-Fermi crossover in Efimov spectrum

In the above discussions, we assumed that two  $A$  particles do not interact with each other. The presence of a short-range interaction between  $A$  particles modifies the spectrum of  $AAB$  Efimov trimers. Suppose  $A$  particles are bosons and interact with each other via a zero-range potential with finite scattering length  $a$ , in addition to the infinite scattering length interaction with one  $B$  particle. Because  $a$  introduces a scale, the spectrum of  $AAB$  trimers  $\{E_n\}$  is no longer given by Eq. (1). For deep trimers whose size  $\sim \kappa_n^{-1} \equiv \hbar/\sqrt{2\mu|E_n|}$  is much smaller than  $|a|$ , the scattering length can be regarded as effectively infinite  $a \rightarrow \infty$ . Because the scale  $a$  disappears in such a limit, the spectrum of trimers exhibits the approximate discrete scaling symmetry with a certain scaling factor  $\lambda_{\text{uv}}$  due to the Efimov effect. On the other hand, for shallow trimers whose size  $\sim \kappa_n^{-1}$  is much larger than  $|a|$ , the scattering length can be regarded as effectively vanishing  $a \rightarrow 0$ . Because the scale  $a$  disappears in such a limit again, the spectrum of trimers exhibits the approximate discrete scaling symmetry but with a different scaling factor  $\lambda_{\text{ir}}$ . Therefore, the spectrum of  $AAB$  trimers shows an intriguing crossover from the ultraviolet scaling behavior

$$\frac{E_{n+1}}{E_n} \approx \lambda_{\text{uv}}^{-2} \quad \text{for} \quad \frac{1}{\kappa_n|a|} \ll 1 \quad (18)$$

to the infrared scaling behavior

$$\frac{E_{n+1}}{E_n} \approx \lambda_{\text{ir}}^{-2} \quad \text{for} \quad \frac{1}{\kappa_n|a|} \gg 1. \quad (19)$$

In a terminology of the renormalization group, this is a crossover from the ultraviolet limit cycle governed by  $a \rightarrow \infty$  to the infrared limit cycle governed by  $a \rightarrow 0$ . If the Efimov effect does not take place in the limit  $a \rightarrow 0$  which corresponds to  $\lambda_{\text{ir}} \rightarrow \infty$ , the Efimov spectrum of trimers in Eq. (18) will terminate around  $\kappa_n|a| \sim 1$ .

We demonstrate this general consideration by taking a particularly interesting example in which two  $A$  bosons are confined in 1D and resonantly interact with one  $B$  particle in 3D. The zero-range potential between  $A$  bosons is given by

$$V_A(z) = g_{1\text{D}} \delta(z) \quad \text{with} \quad g_{1\text{D}} \equiv -\frac{2\hbar^2}{m_A a_{1\text{D}}}, \quad (20)$$

where  $a_{1\text{D}} < 0$  is the 1D scattering length. At infinite scattering length  $a_{1\text{D}} \rightarrow \infty$ , the coupling vanishes  $g_{1\text{D}} \rightarrow 0$  and thus two  $A$  bosons are noninteracting. Therefore, the ultraviolet scaling factor  $\lambda_{\text{uv}} = e^{\pi/s_{\text{uv}}}$  is simply obtained from the exponent  $s_{\text{uv}} = s_0$  for noninteracting  $A$  bosons, which is already plotted in the left panel of Fig. 1 (dotted curve) as a function of the mass ratio  $m_A/m_B$ . On the other hand, at zero scattering length  $a_{1\text{D}} \rightarrow -0$ , the coupling diverges  $g_{1\text{D}} \rightarrow +\infty$  and thus the potential  $V_A(z)$  becomes a hardcore repulsion. Since the spectrum of bosons interacting via the hardcore repulsion in 1D is equivalent to that of noninteracting identical fermions [15], the infrared scaling factor  $\lambda_{\text{ir}} = e^{\pi/s_{\text{ir}}}$  is obtained from the exponent  $s_{\text{ir}} = s_1$  for noninteracting  $A$  “fermions”, which is also already plotted in the right panel of Fig. 1 (dotted curve).

Figure 3 shows the ratio of two successive binding energies  $\sqrt{E_n/E_{n+1}} = \kappa_n/\kappa_{n+1}$  in the even-parity channel as a function of  $1/(\kappa_n|a_{1\text{D}}|)$  for two mass ratios  $m_A/m_B = 41/6$  (left panel) and  $m_A/m_B = 41/40$  (right panel), corresponding to  $A = {}^{41}\text{K}$ ,  $B = {}^6\text{Li}$  and  $A = {}^{41}\text{K}$ ,  $B = {}^{40}\text{K}$ , respectively (see Appendix A for details). In the former case of  $m_A/m_B = 41/6$ , the spectrum of  $AAB$  trimers shows the crossover from the bosonic scaling behavior

$$\frac{\kappa_n}{\kappa_{n+1}} \approx 13.3 \quad \text{for} \quad \frac{1}{\kappa_n|a_{1\text{D}}|} \ll 1 \quad (21)$$

to the fermionic scaling behavior

$$\frac{\kappa_n}{\kappa_{n+1}} \approx 21.0 \quad \text{for} \quad \frac{1}{\kappa_n|a_{1\text{D}}|} \gg 1. \quad (22)$$



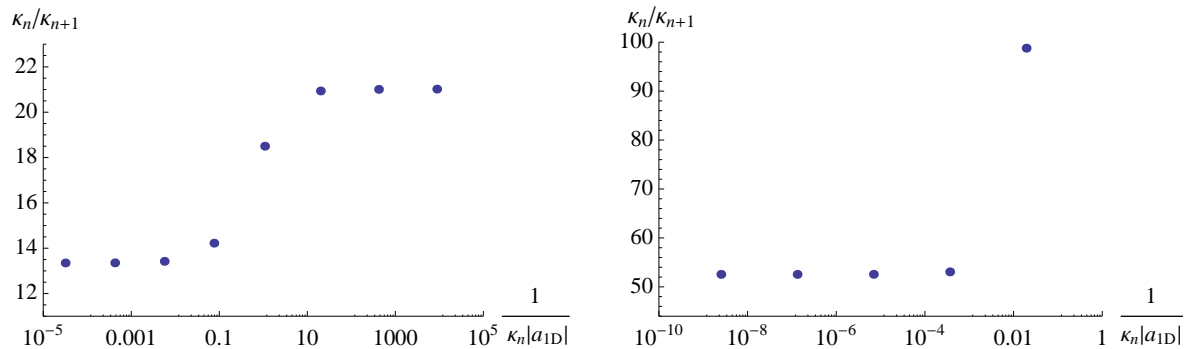


**Fig. 3** Bose-Fermi crossover in ratios of two successive binding energies  $\sqrt{E_n/E_{n+1}} = \kappa_n/\kappa_{n+1}$  of  $AAB$  trimers in the even-parity channel as functions of  $1/(\kappa_n|a_{1D}|)$ . The left and right panels are for mass ratios  $m_A/m_B = 41/6$  and  $m_A/m_B = 41/40$ , respectively, and the 1D scattering length is chosen as  $a_{1D} = -\kappa_*^{-1}$ , where  $\kappa_*$  is the Efimov parameter in the noninteracting limit  $a_{1D} \rightarrow \infty$  [see Eq. (39)].

On the other hand, in the latter case of  $m_A/m_B = 41/40$ , the Efimov spectrum of trimers

$$\frac{\kappa_n}{\kappa_{n+1}} \approx 52.5 \quad \text{for} \quad \frac{1}{\kappa_n|a_{1D}|} \ll 1 \quad (23)$$

terminates around  $\kappa_n|a_{1D}| \sim 1$  because the mass ratio is below the critical value of  $m_A/m_B = 2.06$  for  $A$  “fermions”. This new phenomenon, *Bose-Fermi crossover* in the Efimov spectrum, is unique in our 1D-3D mixture and will be in principle observable in ultracold atom experiments.

#### 4.3 Interlayer Efimov trimers and stability in ultracold atoms [32]

Efimov trimers realized in ultracold atoms are unstable due to the three-body recombination decaying into deeply bound dimers (see, for example [33]). This would be a part of the reasons why the spectroscopy of the Efimov trimers has not been performed in ultracold atom experiments with the exception of recent Refs. [34, 35]. The idea of mixed dimensions is useful to realize stable Efimov trimers in ultracold atoms.

In order for an  $AAB$  trimer to decay into a deeply bound  $AB$  dimer with an  $A$  atom, all three atoms have to come within a narrow range of the interatomic potential  $\sim r_0$ . This inelastic three-body collision can be prevented by spatially separating two  $A$  atoms by a distance larger than  $r_0$ . Therefore, we consider to confine two  $A$  particles in two parallel 2D planes or 1D lines separated by a distance  $d$  and let them interact with one  $B$  particle placed in 3D. By making  $d \gg r_0$  and neglecting the interlayer or interwire tunneling, the  $AAB$  system becomes stable against the three-body recombination. Furthermore, when the short-range interaction between  $A$  and  $B$  particles is resonant, two  $A$  and one  $B$  particles always form an infinite tower of bound states even if two  $A$  particles are spatially separated regardless of their statistics and mass ratio. This is because spatially separated  $A$  particles are distinguishable and also because if the size of trimer  $\sim \kappa_n^{-1} \equiv \hbar/\sqrt{2\mu|E_n|}$  is much larger than  $d$ , the separation of two planes or lines can be regarded as effectively vanishing  $d \rightarrow 0$  and thus the problem reduces to the ordinary 2D-3D or 1D-3D mixture where the Efimov effect always appears in the  $s$ -wave or even-parity channel ( $\ell = 0$ ) for any mass ratio as is shown in Sect. 4.1. Therefore, the spectrum of shallow  $AAB$  trimers exhibits the approximate discrete scaling symmetry as

$$\frac{E_{n+1}}{E_n} \approx e^{-2\pi/s_0} \quad \text{for} \quad \kappa_n d \ll 1, \quad (24)$$

where the exponent  $s_0$  is plotted in the left panel of Fig. 1 (dashed or dotted curve) as a function of the mass ratio  $m_A/m_B$ . On the other hand, since two  $A$  particles are spatially separated at least by the distance  $d$ , the size of trimer  $\sim \kappa_n^{-1}$  cannot be smaller than  $d$  and thus the Efimov spectrum of trimers in Eq. (24) has to be terminated by a ground state trimer around  $\kappa_0 d \sim 1$ .

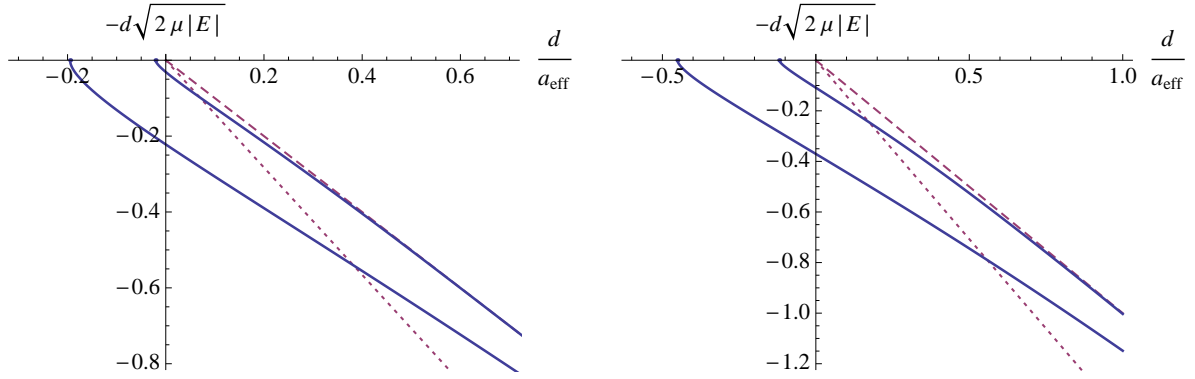


**Fig. 4** Ground state binding energies  $-d\sqrt{2\mu|E_0|/\hbar^2}$  of  $AAB$  trimer in bilayer 2D-3D (left panel) and biwire 1D-3D (right panel) mixtures as functions of the inverse effective scattering length  $d/a_{\text{eff}}$ . The lower and upper solid curves are for mass ratios  $m_A/m_B = 40/6$  and  $m_A/m_B = 6/40$ , respectively, and the dashed and dotted lines are atom-dimer and dimer-dimer thresholds;  $E = -\hbar^2/(2\mu a_{\text{eff}}^2)$  and  $E = -\hbar^2/(\mu a_{\text{eff}}^2)$ .

Figure 4 shows the ground state binding energy  $-d\sqrt{2\mu|E_0|/\hbar^2}$  of  $AAB$  trimer in bilayer 2D-3D (left panel) and biwire 1D-3D (right panel) mixtures as a function of the inverse effective scattering length  $d/a_{\text{eff}}$  for two mass ratios  $m_A/m_B = 40/6$  and  $m_A/m_B = 6/40$ , corresponding to  $A = {}^{40}\text{K}$ ,  $B = {}^6\text{Li}$  and  $A = {}^6\text{Li}$ ,  $B = {}^{40}\text{K}$ , respectively [32] (see Appendix B for details).<sup>3</sup> In particular, the ground state binding energy in the unitarity limit  $a_{\text{eff}} \rightarrow \infty$  is found to be

$$E_0 = -\frac{\hbar^2}{2\mu} \left( \frac{0.222}{d} \right)^2 \quad \text{for} \quad \frac{m_A}{m_B} = \frac{40}{6} \quad (25a)$$

$$E_0 = -\frac{\hbar^2}{2\mu} \left( \frac{0.0310}{d} \right)^2 \quad \text{for} \quad \frac{m_A}{m_B} = \frac{6}{40} \quad (25b)$$

in bilayer 2D-3D mixture and

$$E_0 = -\frac{\hbar^2}{2\mu} \left( \frac{0.370}{d} \right)^2 \quad \text{for} \quad \frac{m_A}{m_B} = \frac{40}{6} \quad (26a)$$

$$E_0 = -\frac{\hbar^2}{2\mu} \left( \frac{0.109}{d} \right)^2 \quad \text{for} \quad \frac{m_A}{m_B} = \frac{6}{40} \quad (26b)$$

in biwire 1D-3D mixture.<sup>4</sup> The ground state trimer in the unitarity limit  $a_{\text{eff}} \rightarrow \infty$  is accompanied by an infinite tower of excited trimer states (not shown in Fig. 4) exhibiting the discrete scaling symmetry as

$$E_{n \gg 1} \approx -\frac{\hbar^2}{2\mu} \left( \frac{0.231}{d} \right)^2 \times (11.3)^{-2n} \quad \text{for} \quad \frac{m_A}{m_B} = \frac{40}{6} \quad (27a)$$

$$E_{n \gg 1} \approx -\frac{\hbar^2}{2\mu} \left( \frac{0.0311}{d} \right)^2 \times (69.3)^{-2n} \quad \text{for} \quad \frac{m_A}{m_B} = \frac{6}{40} \quad (27b)$$

<sup>3</sup> The analog of the scattering length in mixed dimensions is referred to as the effective scattering length  $a_{\text{eff}}$  [17]. In this article, we choose its normalization so that the binding energy of two-body bound state for  $a_{\text{eff}} > 0$  is given by  $E = -\hbar^2/(2\mu a_{\text{eff}}^2)$ . See also Refs. [36,37] in which the different normalization was chosen so that  $E = -\hbar^2/(2m_B a_{\text{eff}}^2)$ .

<sup>4</sup> If we choose  $d = 390 \text{ nm}$  for  $A = {}^{40}\text{K}$  and  $B = {}^6\text{Li}$ , the ground state binding energy is given by  $E_0 = -15.1 \text{ nK} \times k_B$  in bilayer 2D-3D mixture and  $E_0 = -41.9 \text{ nK} \times k_B$  in biwire 1D-3D mixture.

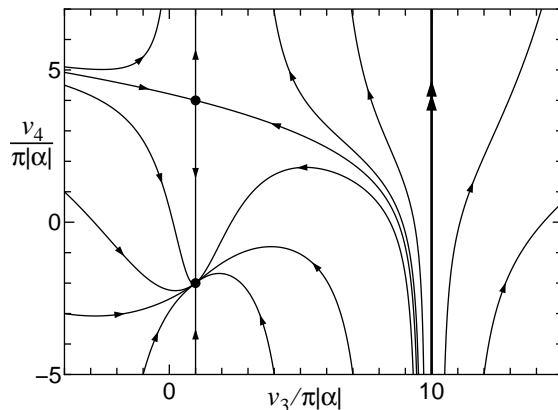


**Fig. 5** Renormalization group flow diagram in the plane of three-body and four-body couplings,  $v_3$  and  $v_4$ , when the two-body interaction is tuned to the two-body resonance  $a \rightarrow \infty$  [16]. If the three-body interaction is tuned to the ultraviolet fixed point at  $v_3 = 10\pi|\alpha|$  corresponding to the three-body resonance, the four-body coupling  $v_4$  exhibits the limit cycle (thick line with two arrows) indicating the Efimov effect in four anyons.

in bilayer 2D-3D mixture and

$$E_{n \gg 1} \approx -\frac{\hbar^2}{2\mu} \left( \frac{0.399}{d} \right)^2 \times (13.6)^{-2n} \quad \text{for} \quad \frac{m_A}{m_B} = \frac{40}{6} \quad (28a)$$

$$E_{n \gg 1} \approx -\frac{\hbar^2}{2\mu} \left( \frac{0.109}{d} \right)^2 \times (76.6)^{-2n} \quad \text{for} \quad \frac{m_A}{m_B} = \frac{6}{40} \quad (28b)$$

in biwire 1D-3D mixture. Since the interlayer or interwire separation  $d$  is the only scale and plays a role of short-distance cutoff, the spectrum of Efimov trimers that bridge between layers or wires is completely determined by  $d$  (and the effective scattering length  $a_{\text{eff}}$  if finite). Unlike ordinary Efimov trimers in a free space, *these interlayer and interwire Efimov trimers are stable* in ultracold atoms and thus will enable the spectroscopy of the Efimov spectrum in future experiments.

As we have seen above, interlayer or interwire Efimov trimers in the  $s$ -wave or even-parity channel ( $\ell = 0$ ) are always formed for any mass ratio. On the other hand, in the  $p$ -wave or odd-parity channel ( $\ell = 1$ ), they are formed only above a critical mass ratio given by  $m_A/m_B = 6.35$  in bilayer 2D-3D mixture or  $m_A/m_B = 2.06$  in biwire 1D-3D mixture [see Eq. (14)] and the scaling exponent  $s_1$  is plotted in the right panel of Fig. 1 (dashed or dotted curve) as a function of the mass ratio  $m_A/m_B$ . In the case of bilayer 2D-3D mixture, further infinite towers of interlayer Efimov trimers can appear in higher partial-wave channels by increasing  $m_A/m_B$ .

#### 4.4 Resonantly interacting anyons in two dimensions [16]

So far we have discussed the Efimov effect for resonantly interacting bosons and fermions. Here we discuss the possibility of the Efimov effect for anyons in two dimensions. As we have shown below Eq. (9) in Sect. 2, the unitarity limit becomes trivial both for bosons and fermions in two dimensions and thus they cannot exhibit the Efimov effect. On the other hand, the unitarity limit is nontrivial for anyons and thus they may exhibit the Efimov effect.

Ref. [16] developed a perturbation theory to treat anyons attracting via a resonant short-range interaction near the fermionic limit. It was found that unlike bosons in three dimensions, three resonantly interacting anyons do not exhibit the Efimov effect. However, if both two-body and three-body interactions are simultaneously tuned to the two-body and three-body resonances, then the four-body coupling exhibits the renormalization group limit cycle which indicates *the Efimov effect in four anyons* (see Fig. 5). Near the fermionic limit  $|\alpha| \ll 1$ , the ratio of two successive binding energies of four anyons

shows the discrete scaling symmetry as

$$\frac{E_{n+1}}{E_n} = \exp\left[-\frac{2\pi}{6|\alpha| + O(\alpha^2)}\right], \quad (29)$$

where  $\alpha$  is the statistics parameter defined so that  $\alpha = 0$  corresponds to fermions and  $|\alpha| = 1$  corresponds to bosons. On the other hand, anyons near the bosonic limit  $|\alpha| \rightarrow 1$  do not exhibit the Efimov effect. Therefore, the infinite tower of four-anyon bound states found near the fermionic limit  $|\alpha| \ll 1$  has to disappear at a certain critical value of  $0 < |\alpha| < 1$ .

## 5 Summary

The Efimov physics has been studied for more than 40 years and considered to exist only in three dimensions. In this article, we reviewed how the Efimov physics can be liberated from three dimensions. We elucidated that scale-invariant interactions are necessary for the Efimov effect and found that two-body and three-body interactions in mixed dimensions and four-body interaction in one dimension become scale invariant in the unitarity limit. Then by adding another particle, all such new systems indeed exhibit the Efimov effect. Complete and unified analyses of the Efimov effect in all possible cases will be presented in a separate paper [12]. Here we focused on a number of universal phenomena, such as confinement-induced Efimov effect, Bose-Fermi crossover in Efimov spectrum, and formation of interlayer Efimov trimers, that are unique in our new systems and observable in ultracold atom experiments. We also discussed the Efimov effect for anyons in two dimensions. Therefore, we can find the Efimov effect in all spatial dimensions; three bosons with a resonant two-body interaction in 3D [2], four anyons with resonant two-body and three-body interactions in 2D [16], five bosons with a resonant four-body interaction in 1D [38], and various mixed-dimensional systems [17]. An important first step toward Efimov physics beyond three dimensions has been recently taken by the experimental group at Florence [39]. They realized the 2D-3D mixed dimensions by using the ultracold Bose-Bose mixture of  $^{41}\text{K}$  in 2D and  $^{87}\text{Rb}$  in 3D and observed a series of two-body scattering resonances where the Efimov effect is supposed to appear. In view of the fact that most studies on the Efimov effect have been devoted to three dimensions for more than 40 years, we believe that this study significantly broadens our horizons of universal Efimov physics.

**Acknowledgements** Y. N. was supported by MIT Pappalardo Fellowship in Physics and the U. S. Department of Energy under cooperative research agreement Contract Number DE-FG02-94ER40818.

## A Details of Bose-Fermi crossover in 1D-3D mixture

Here we provide details of the Bose-Fermi crossover in Efimov spectrum discussed in Sect. 4.2. Two  $A$  bosons in 1D interacting with one  $B$  particle in 3D are described by the Schrödinger equation ( $\hbar = 1$ ):

$$\left[-\frac{1}{2m_A} \left(\frac{\partial^2}{\partial z_{A1}^2} + \frac{\partial^2}{\partial z_{A2}^2}\right) - \frac{1}{2m_B} \left(\frac{\partial^2}{\partial z_B^2} + \frac{\partial^2}{\partial \mathbf{x}_B^2}\right) + V\right] \psi(z_{A1}, z_{A2}, z_B, \mathbf{x}_B) = E \psi(z_{A1}, z_{A2}, z_B, \mathbf{x}_B). \quad (30)$$

Here  $\mathbf{x} = (x, y)$  are two-dimensional coordinates and the zero-range potential  $V$  is given by

$$V\psi(z_{A1}, z_{A2}, z_B, \mathbf{x}_B) = \delta(z_B - z_{A1}) \delta\left(\sqrt{\frac{m_B}{\mu}} \mathbf{x}_B\right) f(z_{A1} - z_{A2}) + \delta(z_B - z_{A2}) \delta\left(\sqrt{\frac{m_B}{\mu}} \mathbf{x}_B\right) f(z_{A2} - z_{A1}) \\ + g_{1D} \delta(z_{A1} - z_{A2}) \psi(z_{A1}, z_{A1}, z_B, \mathbf{x}_B). \quad (31)$$

The unknown function  $f$  is defined as

$$f(z_{A1} - z_{A2}) \equiv \frac{2\pi a_{\text{eff}}}{\mu} \lim_{z_B \rightarrow z_{A1}, \mathbf{x}_B \rightarrow \mathbf{0}} \frac{\partial}{\partial R} [R\psi(z_{A1}, z_{A2}, z_B, \mathbf{x}_B)], \quad (32)$$

where  $\mu \equiv m_A m_B / (m_A + m_B)$  is the reduced mass,  $a_{\text{eff}}$  is the effective scattering length, and  $R \equiv \sqrt{(z_B - z_{A1})^2 + \frac{m_B}{\mu} \mathbf{x}_B^2}$  is the “distance” between  $A$  and  $B$  particles [17]. Since the system is translationally invariant in the  $z$  direction, it is convenient to introduce new coordinates

$$z_{12} \equiv z_{A1} - z_{A2}, \quad z_{AB} \equiv z_B - \frac{z_{A1} + z_{A2}}{2}, \quad \text{and} \quad Z \equiv \frac{m_A z_{A1} + m_A z_{A2} + m_B z_B}{2m_A + m_B} \quad (33)$$

and separate the center-of-mass coordinate  $Z$ .

For bound states  $E = -|E| < 0$ , the Schrödinger equation is formally solved by

$$\psi(z_{12}, z_{AB}, \mathbf{x}_B) = - \int dz'_{12} dz'_{AB} d\mathbf{x}'_B \langle z_{12}, z_{AB}, \mathbf{x}_B | \frac{1}{H_0 + |E|} | z'_{12}, z'_{AB}, \mathbf{x}'_B \rangle V \psi(z'_{12}, z'_{AB}, \mathbf{x}'_B). \quad (34)$$

By imposing the short-range boundary condition from Eq. (32)

$$\lim_{z_{AB} \rightarrow \frac{z_{12}^2}{2}, \mathbf{x}_B \rightarrow \mathbf{0}} \psi(z_{12}, z_{AB}, \mathbf{x}_B) = \frac{\mu}{2\pi} \left[ \frac{1}{a_{\text{eff}}} - \frac{1}{R} \right] f(z_{12}) + O(R) \quad (35)$$

and by taking the limit  $z_{12} \rightarrow 0$ , we obtain a set of two integral equations obeyed by  $f(z_{12})$  and  $g(z_{AB}, \mathbf{x}_B) \equiv g_{1D} \psi(0, z_{AB}, \mathbf{x}_B)$ . In the unitarity limit  $a_{\text{eff}} \rightarrow \infty$ , these integral equations in the momentum space are expressed by

$$\begin{aligned} & \frac{\mu}{m_B} \int \frac{dq_z d\mathbf{q}}{(2\pi)^3} \left[ \frac{1}{\frac{(2p_z - q_z)^2}{4m_A} + \frac{2m_A + m_B}{4m_A m_B} q_z^2 + \frac{q^2}{2m_B} + |E|} - \frac{1}{\frac{q_z^2}{2\mu} + \frac{q^2}{2m_B}} \right] f(p_z) \\ &= - \frac{\mu}{m_B} \int \frac{dq_z d\mathbf{q}}{(2\pi)^3} \frac{f(q_z - p_z)}{\frac{(2p_z - q_z)^2}{4m_A} + \frac{2m_A + m_B}{4m_A m_B} q_z^2 + \frac{q^2}{2m_B} + |E|} - \int \frac{dq_z d\mathbf{q}}{(2\pi)^3} \frac{g(q_z, \mathbf{q})}{\frac{(2p_z - q_z)^2}{4m_A} + \frac{2m_A + m_B}{4m_A m_B} q_z^2 + \frac{q^2}{2m_B} + |E|} \end{aligned} \quad (36)$$

and

$$\left[ \frac{1}{g_{1D}} + \int \frac{dq_z}{2\pi} \frac{1}{\frac{q_z^2}{m_A} + \frac{2m_A + m_B}{4m_A m_B} p_z^2 + \frac{p^2}{2m_B} + |E|} \right] g(p_z, \mathbf{p}) = - \frac{2\mu}{m_B} \int \frac{dq_z}{2\pi} \frac{f(q_z + \frac{p_z}{2})}{\frac{q_z^2}{m_A} + \frac{2m_A + m_B}{4m_A m_B} p_z^2 + \frac{p^2}{2m_B} + |E|}. \quad (37)$$

By substituting the solution  $g(p_z, \mathbf{p})$  of the second equation into the first integral equation, we arrive at a closed integral equation obeyed by  $f(p_z)$ :

$$\begin{aligned} \sqrt{\frac{2u+1}{(u+1)^2} p_z^2 + \varepsilon} f(p_z) &= 4\pi \int \frac{dq_z d\mathbf{q}}{(2\pi)^3} \frac{f(q_z)}{p_z^2 + q_z^2 + \frac{2u}{u+1} p_z q_z + q^2 + \varepsilon} \\ &\quad - 16\pi \sqrt{\frac{2}{u+1}} \int \frac{dk_z d\mathbf{k}}{(2\pi)^3} \frac{1}{p_z^2 + \sqrt{\frac{2}{u+1}} p_z k_z + k_z^2 + \mathbf{k}^2 + \frac{u+1}{2} \varepsilon} \\ &\quad \times \frac{1}{|a_{1D}| + \frac{1}{\sqrt{\frac{2u+1}{2u+2} k_z^2 + \mathbf{k}^2 + \frac{u+1}{2} \varepsilon}}} \int \frac{dq_z}{2\pi} \frac{f(q_z)}{q_z^2 + \sqrt{\frac{2}{u+1}} q_z k_z + k_z^2 + \mathbf{k}^2 + \frac{u+1}{2} \varepsilon}, \end{aligned} \quad (38)$$

where we defined  $u \equiv m_A/m_B$  and  $\varepsilon \equiv 2\mu|E|$  and rescaled integration variables to simplify the expression. This integral equation in the even-parity channel  $f(p_z) = f(-p_z)$  has to be solved numerically to find the spectrum of  $AAB$  trimers.

In the noninteracting limit  $a_{1D} \rightarrow \infty$ , we find the Efimov spectrum

$$E_n = - \frac{\hbar^2 \kappa_*^2}{2\mu} \times e^{-2\pi n/s_{\text{uv}}}, \quad (39)$$

where the exponent  $s_{\text{uv}}$  is an imaginary part of the scaling exponent  $\gamma_\ell$  solving the following equation in the even-parity channel ( $\ell = 0$ ):

$$\frac{\sqrt{2u+1}}{u+1} = - \frac{\cos[(\gamma_\ell + 1) \arccos(\frac{u}{u+1})] + (-1)^\ell \cos[(\gamma_\ell + 1) \arccos(\frac{-u}{u+1})]}{(\gamma_\ell + 1) \sin[(\gamma_\ell + 1)\pi]}. \quad (40)$$

On the other hand, in the hardcore limit  $a_{1D} \rightarrow -0$ , we again find the Efimov spectrum

$$E_n = - \frac{\hbar^2 \kappa_*'^2}{2\mu} \times e^{-2\pi n/s_{\text{ir}}}, \quad (41)$$

where the exponent  $s_{\text{ir}}$  is an imaginary part of  $\gamma_\ell$  solving the following equation in the even-parity channel ( $\ell = 0$ ):

$$\frac{\sqrt{2u+1}}{u+1} = \frac{\cos[(\gamma_\ell + 1) \arccos(\frac{u}{u+1})] - (-1)^\ell \cos[(\gamma_\ell + 1) \arccos(\frac{-u}{u+1})]}{(\gamma_\ell + 1) \sin[(\gamma_\ell + 1)\pi]}. \quad (42)$$

We note that the scaling exponent  $\gamma_\ell$  of noninteracting  $A$  fermions satisfies the same equation (42) by exchanging the roles of even and odd parities  $\ell = 0 \leftrightarrow 1$ . Therefore, the hardcore  $A$  bosons have the same energy spectrum as the noninteracting  $A$  “fermions”. When  $0 < |a_{1D}| < \infty$ , the spectrum of  $AA B$  trimers shows the crossover from the bosonic scaling behavior (39) for  $\sqrt{2\mu|E_n|/\hbar^2}|a_{1D}| \gg 1$  to the fermionic scaling behavior (41) for  $\sqrt{2\mu|E_n|/\hbar^2}|a_{1D}| \ll 1$ . This Bose-Fermi crossover can be seen clearly in Fig. 3, where the ratio of two successive binding energies  $\sqrt{E_n/E_{n+1}} = \kappa_n/\kappa_{n+1}$  is plotted as a function of  $1/(\kappa_n|a_{1D}|)$  for two mass ratios  $m_A/m_B = 41/6$  (left panel) and  $m_A/m_B = 41/40$  (right panel) by choosing the 1D scattering length as  $a_{1D} = -\kappa_*^{-1}$ .

## B Details of interlayer and interwire Efimov trimers

Here we provide details of the formation of interlayer and interwire Efimov trimers discussed in Sect. 4.3.

### B.1 Bilayer 2D-3D mixture

Two  $A$  particles in two parallel 2D planes placed at  $z = z_{A1}$  and  $z_{A2}$  interacting with one  $B$  particle in 3D are described by the Schrödinger equation ( $\hbar = 1$ ):

$$\left[ -\frac{1}{2m_A} \left( \frac{\partial^2}{\partial \mathbf{x}_{A1}^2} + \frac{\partial^2}{\partial \mathbf{x}_{A2}^2} \right) - \frac{1}{2m_B} \left( \frac{\partial^2}{\partial \mathbf{x}_B^2} + \frac{\partial^2}{\partial z_B^2} \right) + V \right] \psi(\mathbf{x}_{A1}, \mathbf{x}_{A2}, \mathbf{x}_B, z_B) = E \psi(\mathbf{x}_{A1}, \mathbf{x}_{A2}, \mathbf{x}_B, z_B). \quad (43)$$

Here  $\mathbf{x} = (x, y)$  are two-dimensional coordinates and the zero-range potential  $V$  is given by

$$V\psi(\mathbf{x}_{A1}, \mathbf{x}_{A2}, \mathbf{x}_B, z_B) = \delta(\mathbf{x}_B - \mathbf{x}_{A1}) \delta\left(\sqrt{\frac{m_B}{\mu}}(z_B - z_{A1})\right) f_1(\mathbf{x}_{A1} - \mathbf{x}_{A2}) \\ + \delta(\mathbf{x}_B - \mathbf{x}_{A2}) \delta\left(\sqrt{\frac{m_B}{\mu}}(z_B - z_{A2})\right) f_2(\mathbf{x}_{A2} - \mathbf{x}_{A1}). \quad (44)$$

The unknown functions  $f_1$  and  $f_2$  are defined as

$$f_1(\mathbf{x}_{A1} - \mathbf{x}_{A2}) \equiv \frac{2\pi a_{\text{eff}}}{\mu} \lim_{\mathbf{x}_B \rightarrow \mathbf{x}_{A1}, z_B \rightarrow z_{A1}} \frac{\partial}{\partial R_1} [R_1 \psi(\mathbf{x}_{A1}, \mathbf{x}_{A2}, \mathbf{x}_B, z_B)] \quad (45)$$

and

$$f_2(\mathbf{x}_{A2} - \mathbf{x}_{A1}) \equiv \frac{2\pi a_{\text{eff}}}{\mu} \lim_{\mathbf{x}_B \rightarrow \mathbf{x}_{A2}, z_B \rightarrow z_{A2}} \frac{\partial}{\partial R_2} [R_2 \psi(\mathbf{x}_{A1}, \mathbf{x}_{A2}, \mathbf{x}_B, z_B)], \quad (46)$$

where  $\mu \equiv m_A m_B / (m_A + m_B)$  is the reduced mass,  $a_{\text{eff}}$  is the effective scattering length, and  $R_i \equiv \sqrt{(\mathbf{x}_B - \mathbf{x}_{Ai})^2 + \frac{m_B}{\mu}(z_B - z_{Ai})^2}$  ( $i = 1, 2$ ) is the “distance” between  $A$  and  $B$  particles [17]. Since the system is translationally invariant in the  $x$  and  $y$  directions, it is convenient to introduce new coordinates

$$\mathbf{x}_{12} \equiv \mathbf{x}_{A1} - \mathbf{x}_{A2}, \quad \mathbf{x}_{AB} \equiv \mathbf{x}_B - \frac{\mathbf{x}_{A1} + \mathbf{x}_{A2}}{2}, \quad \text{and} \quad \mathbf{X} \equiv \frac{m_A \mathbf{x}_{A1} + m_A \mathbf{x}_{A2} + m_B \mathbf{x}_B}{2m_A + m_B} \quad (47)$$

and separate the center-of-mass coordinate  $\mathbf{X}$ .

For bound states  $E = -|E| < 0$ , the Schrödinger equation is formally solved by

$$\psi(\mathbf{x}_{12}, \mathbf{x}_{AB}, z_B) = - \int d\mathbf{x}'_{12} d\mathbf{x}'_{AB} dz'_B \langle \mathbf{x}_{12}, \mathbf{x}_{AB}, z_B | \frac{1}{H_0 + |E|} | \mathbf{x}'_{12}, \mathbf{x}'_{AB}, z'_B \rangle V \psi(\mathbf{x}'_{12}, \mathbf{x}'_{AB}, z'_B). \quad (48)$$

By imposing the short-range boundary conditions from Eq. (45)

$$\lim_{\mathbf{x}_{AB} \rightarrow \frac{\mathbf{x}_{12}}{2}, z_B \rightarrow z_{A1}} \psi(\mathbf{x}_{12}, \mathbf{x}_{AB}, z_B) = \frac{\mu}{2\pi} \left[ \frac{1}{a_{\text{eff}}} - \frac{1}{R_1} \right] f_1(\mathbf{x}_{12}) + O(R_1) \quad (49)$$

and from Eq. (46)

$$\lim_{\mathbf{x}_{AB} \rightarrow -\frac{\mathbf{x}_{12}}{2}, z_B \rightarrow z_{A2}} \psi(\mathbf{x}_{12}, \mathbf{x}_{AB}, z_B) = \frac{\mu}{2\pi} \left[ \frac{1}{a_{\text{eff}}} - \frac{1}{R_2} \right] f_2(-\mathbf{x}_{12}) + O(R_2), \quad (50)$$

we obtain a set of two integral equations obeyed by  $f_1(\mathbf{x}_{12})$  and  $f_2(\mathbf{x}_{12})$ . These integral equations in the momentum space are expressed by

$$\begin{aligned} & \left[ \frac{\mu}{2\pi a_{\text{eff}}} + \sqrt{\frac{\mu}{m_B}} \int \frac{d\mathbf{q}dq_z}{(2\pi)^3} \left( \frac{1}{\frac{(2\mathbf{p}-\mathbf{q})^2}{4m_A} + \frac{2m_A+m_B}{4m_A m_B} \mathbf{q}^2 + \frac{q_z^2}{2m_B} + |E|} - \frac{1}{\frac{q^2}{2\mu} + \frac{q_z^2}{2m_B}} \right) \right] f_1(\mathbf{p}) \\ &= -\sqrt{\frac{\mu}{m_B}} \int \frac{d\mathbf{q}dq_z}{(2\pi)^3} \frac{e^{iq_z(z_{A1}-z_{A2})}}{\frac{(2\mathbf{p}-\mathbf{q})^2}{4m_A} + \frac{2m_A+m_B}{4m_A m_B} \mathbf{q}^2 + \frac{q_z^2}{2m_B} + |E|} f_2(\mathbf{q}-\mathbf{p}) \end{aligned} \quad (51)$$

and  $1 \leftrightarrow 2$ . By defining  $f_{\pm} = f_1 \pm f_2$ , we arrive at a closed integral equation obeyed by  $f_{\pm}(\mathbf{p})$ :

$$\left[ \sqrt{\frac{2u+1}{(u+1)^2} p^2 + \varepsilon} - \frac{1}{a_{\text{eff}}} \right] f_{\pm}(\mathbf{p}) = \pm \int \frac{d\mathbf{q}}{2\pi} \frac{e^{-d\sqrt{\frac{u+1}{u}} \sqrt{p^2+q^2+\frac{2u}{u+1}\mathbf{p}\cdot\mathbf{q}+\varepsilon}}}{\sqrt{p^2+q^2+\frac{2u}{u+1}\mathbf{p}\cdot\mathbf{q}+\varepsilon}} f_{\pm}(\mathbf{q}), \quad (52)$$

where we defined  $u \equiv m_A/m_B$ ,  $\varepsilon \equiv 2\mu|E|$ , and the interlayer separation  $d \equiv |z_{A1} - z_{A2}|$ . Finally, the partial-wave projection  $f_{\pm}^{(\ell)}(\mathbf{p}) \equiv \int_0^\pi \frac{d\varphi}{\pi} \cos(\ell\varphi) f_{\pm}(\mathbf{p})$  leads to

$$\left[ \sqrt{\frac{2u+1}{(u+1)^2} p^2 + \varepsilon} - \frac{1}{a_{\text{eff}}} \right] f_{\pm}^{(\ell)}(\mathbf{p}) = \pm \int_0^\infty dq q \int_0^\pi \frac{d\varphi}{\pi} \cos(\ell\varphi) \frac{e^{-d\sqrt{\frac{u+1}{u}} \sqrt{p^2+q^2+\frac{2u \cos \varphi}{u+1} p q + \varepsilon}}}{\sqrt{p^2+q^2+\frac{2u \cos \varphi}{u+1} p q + \varepsilon}} f_{\pm}^{(\ell)}(\mathbf{q}). \quad (53)$$

The same integral equation has been derived in Ref. [32] by using a field theoretical method. This integral equation for  $f_+^{(\ell)}$  in the  $s$ -wave channel ( $\ell = 0$ ) has been solved numerically to find the spectrum of interlayer  $AAB$  trimers which is plotted as a function of  $d/a_{\text{eff}}$  in the left panel of Fig. 4 for two mass ratios  $m_A/m_B = 40/6$  and  $m_A/m_B = 6/40$ .

## B.2 Biwire 1D-3D mixture

The case for two  $A$  particles in two parallel 1D lines placed at  $\mathbf{x} = \mathbf{x}_{A1}$  and  $\mathbf{x}_{A2}$  interacting with one  $B$  particle in 3D can be studied in the same way by exchanging the roles of above  $\mathbf{x} \leftrightarrow z$ . The resulting integral equation obeyed by  $f_{\pm}(p_z) \equiv f_1(p_z) \pm f_2(p_z)$  is

$$\left[ \sqrt{\frac{2u+1}{(u+1)^2} p_z^2 + \varepsilon} - \frac{1}{a_{\text{eff}}} \right] f_{\pm}(p_z) = \pm \int_{-\infty}^{\infty} \frac{dq_z}{\pi} K_0 \left( d \sqrt{\frac{u+1}{u}} \sqrt{p_z^2 + q_z^2 + \frac{2u}{u+1} p_z q_z + \varepsilon} \right) f_{\pm}(q_z), \quad (54)$$

where we defined the interwire separation  $d \equiv |\mathbf{x}_{A1} - \mathbf{x}_{A2}|$ . This integral equation for  $f_+$  in the even-parity channel  $f(p_z) = f(-p_z)$  has been solved numerically to find the spectrum of interwire  $AAB$  trimers which is plotted as a function of  $d/a_{\text{eff}}$  in the right panel of Fig. 4 for two mass ratios  $m_A/m_B = 40/6$  and  $m_A/m_B = 6/40$ .

## References

1. E. Braaten and H.-W. Hammer, ‘‘Universality in few-body systems with large scattering length,’’ Phys. Rept. **428**, 259 (2006) [arXiv:cond-mat/0410417].
2. V. Efimov, ‘‘Energy levels arising from resonant two-body forces in a three-body system,’’ Phys. Lett. **33B**, 563 (1970); ‘‘Energy levels of three resonantly interacting particles,’’ Nucl. Phys. A **210**, 157 (1973).
3. P. F. Bedaque, H. W. Hammer, and U. van Kolck, ‘‘Renormalization of the three-body system with short range interactions,’’ Phys. Rev. Lett. **82**, 463-467 (1999) [arXiv:nucl-th/9809025]; ‘‘The Three boson system with short range interactions,’’ Nucl. Phys. **A646**, 444-466 (1999) [arXiv:nucl-th/9811046].
4. L. W. Bruch and J. A. Tjon, ‘‘Binding of three identical bosons in two dimensions,’’ Phys. Rev. A **19**, 425 (1979).
5. T. K. Lim and P. A. Maurone, ‘‘Nonexistence of the Efimov effect in two dimensions,’’ Phys. Rev. B **22**, 1467 (1980).
6. T. K. Lim and B. Shimer, ‘‘The Fonseca-Redish-Shanley solvable model for a molecular three-body system and the efimov effect in two dimensions,’’ Z. Phys. A **297**, 185 (1980).

- 
7. S. A. Vugal'ter and G. M. Zhislin, "On the discrete spectrum of the energy operator of one- and two-dimensional quantum three-particle systems," *Theor. Math. Phys.* **55**, 493 (1983).
  8. S. K. Adhikari, W. G. Gibson, and T. K. Lim, "Effective-range theory in two dimensions," *J. Chem. Phys.* **85**, 5580 (1986).
  9. S. K. Adhikari, A. Delfino, T. Frederico, I. D. Goldman, and L. Tomio, "Efimov and Thomas effects and the model dependence of three-particle observables in two and three dimensions," *Phys. Rev. A* **37**, 3666 (1988).
  10. E. Nielsen, D. V. Fedorov, and A. S. Jensen, "Three-body halos in two dimensions," *Phys. Rev. A* **56**, 3287 (1997) [arXiv:quant-ph/9708025]; "Structure and Occurrence of Three-Body Halos in Two Dimensions," *Few-Body Syst.* **27**, 15 (1999).
  11. E. Nielsen, D. V. Fedorov, A. S. Jensen, and E. Garrido, "The three-body problem with short-range interactions," *Phys. Rept.* **347**, 373 (2001).
  12. S. Tan and Y. Nishida, "Geometrical Pictures of Few-Body Systems with a Single Type of Resonance," in preparation.
  13. Z. Nussinov and S. Nussinov, "Triviality of the BCS-BEC crossover in extended dimensions: Implications for the ground state energy," *Phys. Rev. A* **74**, 053622 (2006) [arXiv:cond-mat/0410597].
  14. Y. Nishida and D. T. Son, "Unitary Fermi gas,  $\epsilon$  expansion, and nonrelativistic conformal field theories," arXiv:1004.3597 [cond-mat.quant-gas], to appear in *BCS-BEC crossover and the Unitary Fermi Gas*, edited by W. Zwerger (Lecture Notes in Physics, Springer, 2011).
  15. M. Girardeau, "Relationship between systems of impenetrable bosons and fermions in one dimension," *J. Math. Phys.* **1**, 516 (1960).
  16. Y. Nishida, "Renormalization group analysis of resonantly interacting anyons," *Phys. Rev. D* **77**, 061703 (2008) [arXiv:0708.4056 (hep-th)].
  17. Y. Nishida and S. Tan, "Universal Fermi gases in mixed dimensions," *Phys. Rev. Lett.* **101**, 170401 (2008) [arXiv:0806.2668 (cond-mat.other)].
  18. Y. Nishida and S. Tan, "Confinement-induced Efimov resonances in Fermi-Fermi mixtures," *Phys. Rev. A* **79**, 060701 (2009) [arXiv:0903.3633 (cond-mat.other)].
  19. S. Tan, "Short Range Scaling Laws of Quantum Gases With Contact Interactions," arXiv:cond-mat/0412764.
  20. F. Werner and Y. Castin, "The unitary three-body problem in a trap," *Phys. Rev. Lett.* **97**, 150401 (2006) [arXiv:cond-mat/0507399]; "The unitary gas in an isotropic harmonic trap: symmetry properties and applications," *Phys. Rev. A* **74**, 053604 (2006) [arXiv:cond-mat/0607821].
  21. Y. Nishida and D. T. Son, "Nonrelativistic conformal field theories," *Phys. Rev. D* **76**, 086004 (2007) [arXiv:0706.3746 (hep-th)].
  22. G. Barontini, C. Weber, F. Rabatti, J. Catani, G. Thalhammer, M. Inguscio, and F. Minardi, "Observation of Heteronuclear Atomic Efimov Resonances," *Phys. Rev. Lett.* **103**, 043201 (2009); *ibid.* **104**, 059901(E) (2010) [arXiv:0901.4584 (cond-mat.other)].
  23. D. S. Petrov, "Three-body problem in Fermi gases with short-range interparticle interaction," *Phys. Rev. A* **67**, 010703(R) (2003) [arXiv:cond-mat/0209246].
  24. M. Taglieber, A.-C. Voigt, T. Aoki, T. W. Hänsch, and K. Dieckmann, "Quantum Degenerate Two-Species Fermi-Fermi Mixture Coexisting with a Bose-Einstein Condensate," *Phys. Rev. Lett.* **100**, 010401 (2008) [arXiv:0710.2779 (cond-mat.other)].
  25. E. Wille, F. M. Spiegelhalder, G. Kerner, D. Naik, A. Trenkwalder, G. Hendl, F. Schreck, R. Grimm, T. G. Tiecke, J. T. M. Walraven, S. J. J. M. F. Kokkelmans, E. Tiesinga, and P. S. Julienne, "Exploring an Ultracold Fermi-Fermi Mixture: Interspecies Feshbach Resonances and Scattering Properties of 6Li and 40K," *Phys. Rev. Lett.* **100**, 053201 (2008) [arXiv:0711.2916 (cond-mat.other)].
  26. A.-C. Voigt, M. Taglieber, L. Costa, T. Aoki, W. Wieser, T. W. Hänsch, and K. Dieckmann, "Ultracold Heteronuclear Fermi-Fermi Molecules," *Phys. Rev. Lett.* **102**, 020405 (2009) [arXiv:0810.1306 (cond-mat.other)].
  27. T. G. Tiecke, M. R. Goosen, A. Ludewig, S. D. Gensemer, S. Kraft, S. J. J. M. F. Kokkelmans, and J. T. M. Walraven, "Broad Feshbach Resonance in the 6Li-40K Mixture," *Phys. Rev. Lett.* **104**, 053202 (2010) [arXiv:0908.2071 (cond-mat.quant-gas)].



- 
28. D. Naik, A. Trenkwalder, C. Kohstall, F. M. Spiegelhalter, M. Zaccanti, G. Hendl, F. Schreck, R. Grimm, T. M. Hanna, and P. S. Julienne, “Feshbach resonances in the 6Li-40K Fermi-Fermi mixture: Elastic versus inelastic interactions,” arXiv:1010.3662 [cond-mat.quant-gas].
  29. A. Trenkwalder, C. Kohstall, M. Zaccanti, D. Naik, A. I. Sidorov, F. Schreck, and R. Grimm, “Hydrodynamic Expansion of a Strongly Interacting Fermi-Fermi Mixture,” Phys. Rev. Lett. **106**, 115304 (2011) [arXiv:1011.5192 (cond-mat.quant-gas)].
  30. C.-H. Wu, I. Santiago, J. W. Park, P. Ahmadi, and M. W. Zwierlein, “Strongly Interacting Isotopic Bose-Fermi Mixture Immersed in a Fermi Sea,” arXiv:1103.4630 [cond-mat.quant-gas].
  31. J. Levinsen, T. G. Tiecke, J. T. M. Walraven, and D. S. Petrov, “Atom-Dimer Scattering and Long-Lived Trimers in Fermionic Mixtures,” Phys. Rev. Lett. **103**, 153202 (2009) [arXiv:0907.5523 (cond-mat.quant-gas)].
  32. Y. Nishida, “Phases of a bilayer Fermi gas,” Phys. Rev. A **82**, 011605 (2010) [arXiv:0906.4584 (cond-mat.quant-gas)].
  33. F. Ferlaino and R. Grimm, “Forty years of Efimov physics: How a bizarre prediction turned into a hot topic,” Physics **3**, 9 (2010).
  34. T. Lompe, T. B. Ottenstein, F. Serwane, A. N. Wenz, G. Zürn, and S. Jochim, “Radio-Frequency Association of Efimov Trimers,” Science **330**, 940 (2010) [arXiv:1006.2241 (cond-mat.quant-gas)].
  35. S. Nakajima, M. Horikoshi, T. Mukaiyama, P. Naidon, and M. Ueda, “Measurement of an Efimov trimer binding energy in a three-component mixture of 6Li,” arXiv:1010.1954 [cond-mat.quant-gas].
  36. P. Massignan and Y. Castin, “Three-dimensional strong localization of matter waves by scattering from atoms in a lattice with a confinement-induced resonance,” Phys. Rev. A **74**, 013616 (2006) [arXiv:cond-mat/0604232].
  37. Y. Nishida and S. Tan, “Confinement-induced  $p$ -wave resonances from  $s$ -wave interactions,” Phys. Rev. A **82**, 062713 (2010) [arXiv:1011.0033 (cond-mat.quant-gas)].
  38. Y. Nishida and D. T. Son, “Universal four-component Fermi gas in one dimension,” Phys. Rev. A **82**, 043606 (2010) [arXiv:0908.2159 (cond-mat.quant-gas)].
  39. G. Lamporesi, J. Catani, G. Barontini, Y. Nishida, M. Inguscio, and F. Minardi, “Scattering in Mixed Dimensions with Ultracold Gases,” Phys. Rev. Lett. **104**, 153202 (2010) [arXiv:1002.0114 (cond-mat.quant-gas)].